Supporting Information

Budelli et al. 10.1073/pnas.1313433110

SI Materials and Methods

Constructs. Various PCR and subcloning strategies such as genomic PCR amplification of the C terminal of Kv1.4, making annealed linker oligos containing the Kv1.4 minimal tail sequence (Slo1C-Kv-minT), addition of restriction sites and mutated nucleotides via PCR oligos, site-directed mutagenesis using Stratagene's Quick Change Mutagenesis Kit, and overlap extension PCR were used to make the constructs in Fig. 1.

***Xenopus* Oocytes and ND96 Medium for Incubation and Whole-Cell Recording.** Defolliculated *Xenopus* oocytes were injected with 0.5–150 ng of cRNA using a Nanoject II (Drummond Scientific). Injected oocytes were incubated at 18 °C in ND96 complete medium, consisting of ND96 medium plus 2.5 mM sodium pyruvate and penicillin-streptomycin 1 mL/100 mL. The ND96 medium consisted of (in mM) 96 NaCl, 2 KCl, 1.8 $CaCl_2$, 5 $MgCl_2$ 5, and Hepes 5 adjusted to pH 7.5. Currents were recorded 2–5 d after injection.

Electrophysiology and Additional Solutions. Two-microelectrode voltage-clamp (whole-cell) recordings from *Xenopus* oocytes were obtained in ND96 medium with 1 mM 4,4′-diisothiocyanatostilbene-2,2′-disulphonic acid disodium salt hydrate (DIDS) to block the endogenous chloride conductances. The currents were obtained with an Oocyte Clamp OC-725C amplifier (Warner Instrument Corp.). Recordings were obtained by digitizing at 10 kHz, and low-pass filtering was at 1 kHz. The electrodes were made with borosilicate glass capillaries (World Precision Instruments) pulled with a Sutter Instrument Co. P-87 pipette puller and filled with 3 M KCl.

Patch-clamp recordings were acquired with an Axopatch 200B patch clamp (Molecular Devices), digitized at 100 kHz (macroscopic currents) or at 200 kHz (single channel), and were low-pass filtered at 2 kHz for macropatch recording and at 10 kHz for single-channel analysis, unless otherwise indicated. The data were analyzed using pClamp 9 (Molecular Devices), SigmaPlot (Jandel Scientific), Origin (Microcal Software), and custom software for the burst analysis (1).

Solutions for macropatch recordings shown in Figs. 2 *B* and *C*, 3*C*, 4*C*, and 5 and Figs. S2 and S3 *A* and *C* contained in the pipette were (in mM) 140 KMethasulfonate, 1 $MgCl_2$, and 10 Hepes (for symmetrical K^+) or 140 NaMethasulfonate, 10 KMethasulfonate, 1 $MgCl_2$, and 10 Hepes (for asymmetrical K^+). Both pipette solutions were adjusted to pH 7.2 using KOH. The bath (intracellular solution) contained (in mM) 140 KMethasulphonate, 10 Hepes, and 1 EGTA, with $CaCl_2$ and $MgCl_2$ added as needed to obtain the desired free concentrations, adjusted to pH 7.2 with KOH.

For Figs. 3*B* and 4 *A* and *B*, Fig. S1, and Tables S1 and S2, the 0 Ca^{2+} and 0 Mg^{2+} bath (intracellular solution) contained (in mM) 150 KCl, 1 EGTA, 1 EDTA, and 5 mM 2-[(2-Hydroxy-1,1-bis(hydroxymethyl)ethyl)amino]ethanesulfonic acid, N-[Tris (hydroxymethyl)methyl]-2-aminoethanesulfonic acid (TES), with the final solution adjusted to pH 7.0 with KOH. The pipette solution for symmetrical K^+ recording contained (in mM) 150 KCl, 2 mM $MgCl_2$, and 5 TES (pH 7.0). The pipette solution for asymmetric K^+ recording (Fig. 3*B*) was the same as the 0 Ca^{2+} and 0 Mg^{2+} solution, except with 140 mM NaCl and 10 mM KCl. Solutions with symmetrical 150 mM KCl were used unless otherwise indicated. Solutions indicated as 0 Ca^{2+} solutions had calculated free Ca^{2+} <0.01 μM. To this solution sufficient $CaCl_2$ or $MgCl_2$ was added to obtain the calculated free Ca^{2+} and Mg^{2+} levels indicated in the text. Iberiotoxin was from Tocris Bioscience. The other chemicals and reagents were from Sigma-Aldrich.

1. Nimigean CM, Magleby KL (1999) The beta subunit increases the Ca^{2+} sensitivity of large conductance Ca^{2+}-activated potassium channels by retaining the gating in the bursting states. *J Gen Physiol* 113(3):425–440.

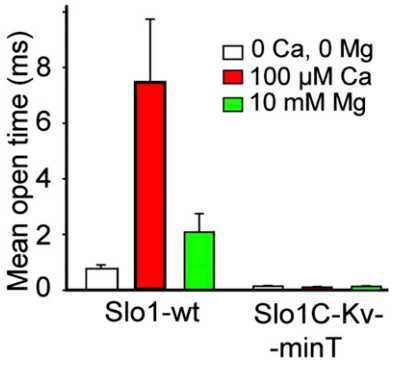

Fig. S1. Ca^{2+} and Mg^{2+} no longer increased the mean open-interval duration (mean open time) after the gating ring in Slo1-WT channels was replaced with an 11-residue tail to obtain Slo1C-Kv-minT channels (see Fig. 1). Data from Table S1 are plotted for Slo1-WT channels and for Slo1C-Kv-minT channels lacking the gating ring. Ca^{2+} and Mg^{2+} significantly increased mean open time for Slo1-WT channels, ($P < 0.05$, paired *t* test, $n = 4$) but had insignificant effects on mean open time for Slo1C-Kv-minT channels ($P > 0.09$, $n = 3$). Symmetrical 150 mM K^+ was used (see *Materials and Methods*). Error bars represent SEM.

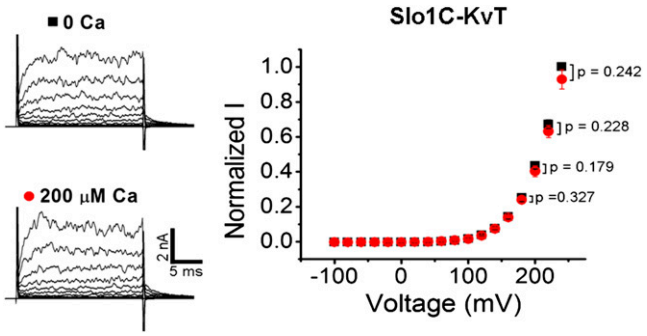

Fig. S2. Slo1C-KvT channels, which lack a gating ring, are activated by voltage but not by Ca^{2+}. Slo1C-KvT channels have the gating ring replaced with a 74-residue tail (Fig. 1). (*Left*) The macroscopic currents were obtained from inside-out patches in asymmetrical K^+ (10 mM K^+ in the pipette and 140 mM K^+ at the inner membrane surface) with either 0 Ca^{2+} or 200 μM Ca^{2+}. Patches were first held at 0 mV. A 50-ms prepulse to −100mV was applied; then the voltage was stepped from −100 mV to 240 mV in 20-mV intervals, followed by a step back to 0 mV to measure outward tail currents. (*Right*) Normalized current amplitudes are plotted against voltage in the absence (black) and presence (red) of Ca^{2+}. Currents were reduced somewhat in the presence of Ca^{2+}, but the reduction was not significant (*P* values are indicated). Error bars represent SEM.

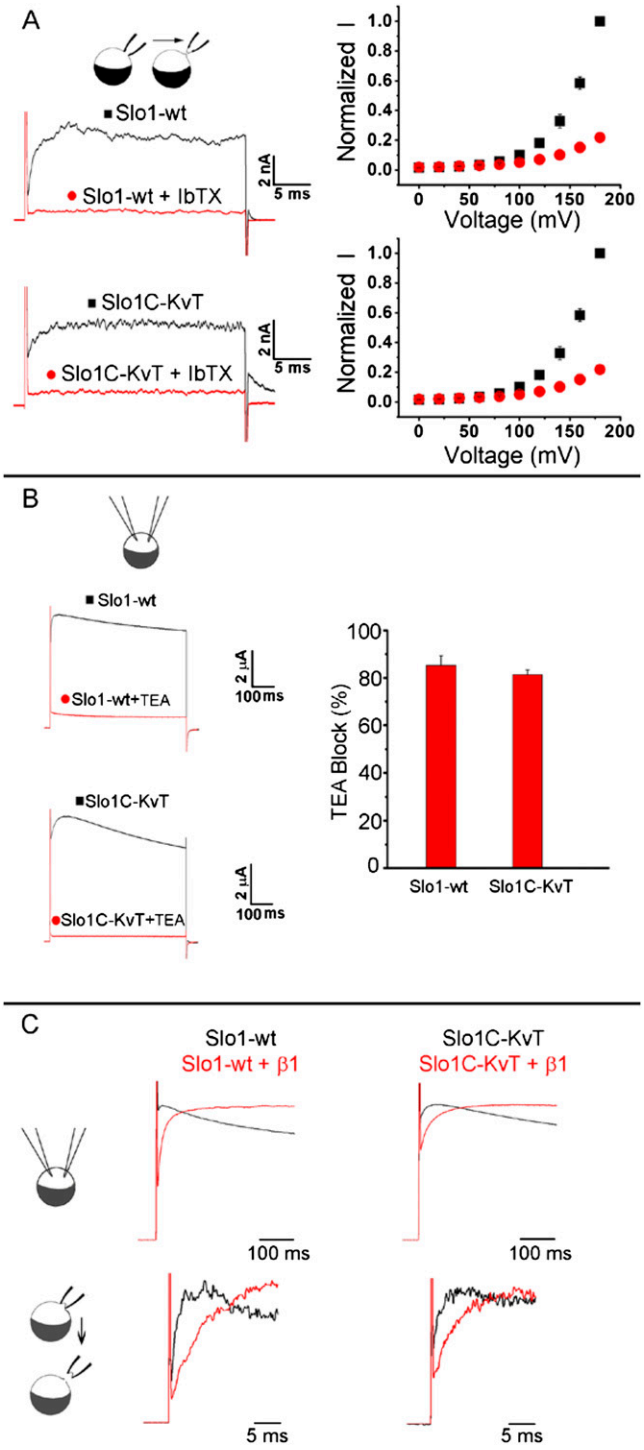

Fig. S3. The gating ring is not required for extracellular block by iberiotoxin (IbTX) or tetraethylammonium (TEA) or for activation by accessory β1 subunits. (*A*) (*Left*) Extracellular application of 60 nM IbTX blocks Slo1-WT and Slo1C-KvT currents similarly in outside-out macropatches. Currents were evoked by stepping from −80 to +180 mV in the absence (black) and presence (red) of 60 nM extracellular IbTX. (*Right*) Normalized I–V plots before (black) and after (red) exposure to IbTX. The blocking effect is virtually the same for Slo1-WT (*Upper*) and Slo1C-KvT (*Lower*) ($n = 6$; $P = 0.42$). (*B*) TEA (2 mM) blocks Slo1-WT and Slo1C-KvT currents in a similar manner. (*Left*) Whole-cell currents evoked at +70 mV before (black) and after (red) 2 mM extracellular TEA. (*Right*) The blocking effect is the same for Slo1-WT and Slo1C-KvT ($n = 6$; $P = 0.32$). (*C*) The auxiliary β1 subunit modulates Slo1-WT and SloC-KvT currents in a similar manner. Coexpression of β1 with Slo1-WT or with Slo1C-KvT slows activation. Red traces are with β1 subunits; black traces are without β1 subunits. Depolarizing pulses are to +60 mV with a two-microelectrode whole-cell voltage clamp (*Upper Left*) and to +240 mV in macropatches (*Lower Left*). The coexpression of β1 significantly slows the activation time constant (τ) for both channel types. The macropatch current rising phase was fitted with a single exponential: Slo1-WT, $\tau = 1.85 \pm 0.28$ ms and 7.26 ± 0.56 ms in the presence of β1 ($P = 0.0001$, $n = 4$); Slo1C-KvT, $\tau = 1.12 \pm 0.07$ ms and 2.94 ± 0.37 ms in the presence of β1 ($P = 0.0006$, $n = 6$). The Slo1C-Kv-MinT construct also was found to be modulated by β1, with a significant threefold change of τ, from 0.91 ± 0.09 ms to 2.61 ± 0.32 ms ($P = 0.001$, $n = 5$). Thus, coexpression with β1 slows the activation of Slo1 constructs with and without the gating ring by about three- to fourfold, indicating that the gating ring is not required for the β1 subunit to slow the activation kinetics. Error bars represent SEM.

Table S1. Single-channel kinetic properties for Slo1-WT and Slo1C-Kv-minT channels in the absence and presence of Ca^{2+} and Mg^{2+}

	Slo1-WT			Slo1C-Kv-minT		
Property	0 Ca^{2+}	100 μM Ca^{2+}	10 mM Mg^{2+}	0 Ca^{2+}	100 μM Ca^{2+}	10 mM Mg^{2+}
nPo	0.0022 ± 0.0008	0.91 ± 0.01	0.13 ± 0.06	0.0037 ± 0.0008	0.0043 ± 0.0011	0.0038 ± 0.0005
Po normalized to 0 Ca	1.0	530 ± 110	53 ± 12	1.0	1.2 ± 0.3	1.2 ± 0.4
No. of openings in bursts	1.5 ± 0.2	28 ± 21	4.8 ± 1.12	1.2 ± 0.1	1.4 ± 0.1	1.5 ± 0.2
Open-interval duration	0.77 ± 0.14	7.5 ± 2.3	2.1 ± 0.66	0.14 ± 0.02	0.11 ± 0.02	0.13 ± 0.02
Intraburst closed-interval duration	0.23 ± 0.03	0.20 ± 0.07	0.16 ± 0.03	0.11 ± 0.03	0.093 ± 0.021	0.14 ± 0.04
Burst duration	1.2 ± 0.2	*	11 ± 5	0.19 ± 0.01	0.17 ± 0.01	0.26 ± 0.06
Mean duration of gaps between bursts	540 ± 100	*	77 ± 25	50 ± 13	34 ± 7	47 ± 4

Data were obtained with single-channel recordings from inside-out patches held at +80 mV. Durations are in milliseconds. Slo1-WT data are from four different patches, each containing a single channel with $n = 1$ in nPo, so that the parameters could be determined readily. Slo1C-Kv-minT data are from three different patches, each containing an unknown number of channels. For Slo1C-Kv-minT channels the mean duration of gaps between bursts for single channels would be greater by a factor of n for the unknown number of channels. For Slo1C-Kv-minT channels the Po was sufficiently low so that openings seldom overlapped; thus the second through fifth parameters could be determined with negligible error. Effective low-pass filtering of 4.47 kHz was used. Data are presented as mean ± SEM. nPo is number of channels in the patch times their average open probability; Po is the average open probability.
*With 100 μM Ca^{2+} for Slo1-WT channels, the Po was so high that the channel was mostly open, so it was difficult to determine gaps between bursts or burst duration.

Table S2. Mean open-interval duration and burst duration are decreased for Slo1C-Kv-minT channels

Property	Slo1-WT	Slo1C-Kv-minT
Open-interval duration	0.77 ± 0.14	0.14 ± 0.02*
No. of opening in bursts	1.5 ± 0.2	1.2 ± 0.1
Intraburst closed-interval duration	0.23 ± 0.03	0.11 ± 0.03
Burst duration	1.2 ± 0.2	0.19 ± 0.01*

Data reformatted from Table S1 to facilitate comparison. Durations are in milliseconds. Data were obtained using single-channel recording with 0 Ca^{2+} and 0 Mg^{2+}. Slo1-WT data are from four different patches, each containing a single channel. Slo1C-Kv-minT data are from three different patches, each containing an unknown number of channels. The Po was sufficiently low so that openings seldom overlapped; thus the parameters could be determined. *Open-interval duration and burst duration were significantly decreased ($P < 0.02$) for Slo1C-Kv-minT channels compared with Slo1-WT channels. Effective low-pass filtering of 4.47 kHz was used. Data are presented as means ± SEM.